

# Wavelet-based Variational Autoencoders for High-Resolution Image Generation

Andrew Kiruluta  
School of Information  
UC Berkeley

April 6, 2025

## Abstract

Variational Autoencoders (VAEs) are powerful generative models capable of learning compact latent representations. However, conventional VAEs often generate relatively blurry images due to their assumption of an isotropic Gaussian latent space and constraints in capturing high-frequency details. In this paper, we explore a novel wavelet-based approach (Wavelet-VAE) in which the latent space is constructed using multi-scale Haar wavelet coefficients. We propose a comprehensive method to encode the image features into multi-scale detail and approximation coefficients and introduce a learnable noise parameter to maintain stochasticity. We thoroughly discuss how to reformulate the reparameterization trick, address the KL divergence term, and integrate wavelet sparsity principles into the training objective. Our experimental evaluation on CIFAR-10 and other high-resolution datasets demonstrates that the Wavelet-VAE improves visual fidelity and recovers higher-resolution details compared to conventional VAEs. We conclude with a discussion of advantages, potential limitations, and future research directions for wavelet-based generative modeling.

## 1 Introduction

Variational Autoencoders (VAEs) [14, 24] are a class of probabilistic generative models that have transformed our ability to learn latent representations for high-dimensional data such as images, text, and audio. By jointly optimizing a differentiable recognition network (the encoder) and a generative model (the decoder), VAEs are capable of mapping complex input data into a lower-dimensional latent space while still maintaining an explicit probabilistic interpretation. However, one of the longstanding challenges in this domain is that conventional VAEs, which often rely on a simple Gaussian prior, can produce outputs that lack sharpness or fine detail, particularly for high-resolution image generation.

### 1.1 Review of Prior VAE Architectures

Since their introduction, VAEs have been extended in numerous ways to address their limitations and improve generative quality. One early development was the importance-weighted autoencoder (IWAE) [2], which refines the evidence lower bound (ELBO) objective by employing multiple samples to produce tighter bounds, leading to improved generation quality. Similarly, hierarchical extensions such as Ladder VAEs [25] and Deep Latent Gaussian Models (DLGMs) [18] aim to capture multi-scale latent representations by stacking multiple layers of latents to facilitate coarse-to-fine image modeling.

Another line of work focuses on enhancing the prior distribution itself. Instead of the standard isotropic Gaussian, Tomczak and Welling [26] proposed the VampPrior, a learnable mixture-of-encoders prior that offers a more expressive latent distribution than a simple Gaussian. Gulrajani et al. [9] introduced PixelVAE, integrating an autoregressive decoder with latent variables to more effectively capture local structures in images. Meanwhile, normalizing flows [23] were incorporated into VAEs to transform

an initially simple prior (like a Gaussian) into more complex distributions through invertible transformations, thereby increasing model expressiveness. VQ-VAE [22] further replaced continuous latent variables with a discrete codebook, yielding sharper reconstructions in image and audio domains.

Hierarchical generative models have also seen rapid progress, with architectures such as NVAE [27] and VDVAE [4], which incorporate deep hierarchical structures of latent variables to improve image fidelity, especially at higher resolutions. Extending VAEs to handle more structured output spaces, DRAW [8] proposed a sequential generative approach that iteratively refines generated images, and VRNN [5] combined VAEs with recurrent neural networks for sequences. Furthermore, specialized designs for tasks like attribute manipulation [29] and text generation [1] underline the versatility of the VAE framework across modalities.

Despite these advances, many VAE variants still rely on Gaussian latents, which can fail to capture subtle local features crucial for high-resolution or complex data distributions. Some solutions, such as multi-layer perceptron (MLP) decoders in the presence of large latent spaces, do achieve improved sharpness in generation [13, 12], but often at the cost of extensive computational resources. Others rely on multi-scale architectures [27, 4], which partly motivates the work we introduce here.

## 1.2 Wavelet-based Approaches for Sharp Reconstructions

Recent trends emphasize learning generative models capable of preserving high-frequency details. Wavelet transforms, being classically lauded for their multi-scale and sparse representations, have appeared as natural candidates in this regard [20, 3]. By decomposing data into coarse approximation and fine detail coefficients, wavelet-based methods can naturally emphasize sharp edges and textures, which is often beneficial in high-resolution image tasks [6, 21]. While many generative models resort to fixed convolutional architectures [7], wavelet-based networks directly incorporate frequency analysis into their design, potentially enhancing interpretability and efficient representation learning [19].

Our proposed approach, the Wavelet-VAE, seeks to unify the theoretical strengths of VAEs with the practical advantages offered by wavelet transforms. In particular, by treating wavelet coefficients as the latent variables, we leverage the inherent sparsity and multi-scale nature of wavelets to mitigate the notorious blur often observed in conventional VAE outputs. Additionally, applying sparsity-inducing regularization (or a KL-like penalty) on wavelet coefficients encourages the model to learn compressed yet informative representations, thereby improving generalization and interpretability [28, 10].

In this work, we propose a Wavelet-based Variational Autoencoder (Wavelet-VAE) that leverages multi-scale Haar wavelet coefficients as the latent representation [16, 15], replacing the conventional Gaussian assumption. This approach enhances the model’s capacity to capture high-frequency structures and significantly mitigates the blurred reconstructions commonly found in standard VAEs. Furthermore, by introducing a learnable noise scale for the wavelet coefficients, our model adaptively balances stochasticity and fidelity in the latent space. Below, we provide an in-depth look at the fundamental components of VAEs and how wavelet transforms can overcome inherent limitations in conventional setups. More recently, Haar based Wavelet transforms have been successfully employed in the next generation of condition stable diffusion models to synthesize high-quality, high-fidelity images with improved spatial localization [16].

## 1.3 Contributions and Overview

In this work, we present a comprehensive study of the Wavelet-VAE architecture. We thoroughly detail the mathematical foundations for shifting from a standard Gaussian latent space to one composed of hierarchical Haar wavelet coefficients. We also incorporate learnable noise parameters to control stochasticity and preserve the essential reparameterization trick of VAEs. Our methodology demonstrates empirically superior results on high-resolution image benchmarks, including CIFAR-10 [17] and CelebA-HQ [11], achieving both lower reconstruction error and sharper outputs. We discuss the mathematical underpinnings (Section 3), delve into our Wavelet-VAE architecture (Section ??), and provide extensive quantitative and qualitative experiments (Section 4). We conclude with a discussion of broader

impacts, limitations, and potential future avenues in leveraging wavelet-based representation learning for high-fidelity image synthesis.

Overall, our research aims to bridge the gap between the theoretical elegance of wavelet transforms and the practical requirements of large-scale generative modeling, furthering the capacity of VAEs to produce high-quality, high-resolution images. We believe that the success of the Wavelet-VAE underscores the promise of structured latent representations, paving the way for more interpretable, flexible, and effective generative models.

## 1.4 Overview of Variational Autoencoders

Variational Autoencoders (VAEs) [14, 24] constitute a popular class of deep generative models that learn to map high-dimensional data (e.g., images) to lower-dimensional latent representations from which data can be sampled or reconstructed. The VAE framework consists of two key components:

- **Encoder (Inference Network):** This network takes an input (e.g., an image) and outputs parameters of an approximate posterior distribution over the latent variable. Typically, the parameters correspond to a mean and variance for a Gaussian distribution.
- **Decoder (Generative Network):** Given a latent sample, the decoder aims to reconstruct the original data by modeling.

What distinguishes the VAE from older latent variable models is the reparameterization trick, which re-expresses the sampling operation in a way that permits end-to-end backpropagation. This innovation made it possible to train large-scale generative models by gradient-based optimization techniques.

## 1.5 Limitations of Conventional VAE Approaches

While VAEs allow for meaningful latent-space operations and stable training, they often produce blurry or over-smoothed images. Two primary factors are typically cited:

1. **Gaussian Latent Prior:** A simple Gaussian prior may be insufficiently expressive to encapsulate all the rich structure in complex image distributions. Consequently, the model focuses on broad, low-frequency features, neglecting high-frequency details.
2. **Pixel-wise Reconstruction Losses:** Mean Squared Error (MSE) or pixel-wise cross-entropy penalizes large deviations but is tolerant of small, distributed errors across the entire image, leading to a smooth, averaged outcome.

Efforts to address these shortcomings have included alternative priors, hierarchical latent variables, or more perceptual-based reconstruction metrics. Nonetheless, there remains a gap in capturing localized high-frequency details inherent in natural images.

## 1.6 Motivation for Wavelet-based Latent Representations

Wavelet transforms [20] decompose signals into localized basis functions, offering a natural multi-scale representation of images. This framework presents several attractive properties for VAE-like models:

- **Multi-scale Decomposition:** Images can be separated into coarse approximation coefficients and finer detail coefficients across multiple scales.
- **Local Frequency Analysis:** Wavelets encode localized frequency components, allowing sharper reconstructions of edges and textures.
- **Sparsity:** In many real-world images, wavelet representations tend to be sparse, which can be leveraged to improve generalization.

Replacing the Gaussian latent space with wavelet coefficients thus holds the promise of higher-resolution reconstructions and better fidelity, especially in capturing high-frequency structures. As we shall see, introducing a learnable noise scale helps maintain the stochastic component of a VAE, further refining performance and flexibility.

## 1.7 Multi-scale Generative Models

Several multi-scale generative models have attempted to incorporate hierarchical representations, such as progressive GANs [11] or hierarchical VAEs [27]. These models typically aim to learn coarse-to-fine image structure, which aligns with the wavelet concept. However, explicit wavelet decomposition within the latent space has not been explored as extensively.

## 1.8 VAEs with Advanced Priors

Another line of research modifies the prior distribution beyond simple Gaussians, such as VampPrior [26] or autoregressive priors [9]. While these methods can capture more complex distributions, they often require large parametric overhead or sophisticated coupling. By contrast, a wavelet-based approach provides a structured, multi-scale alternative with potentially lower overhead.

# 2 Related Work

## 2.1 Wavelets in Deep Learning

Wavelet transforms have a long history in signal processing and computer vision, originating from the need for effective signal and image compression and denoising techniques. Their ability to capture localized spatial-frequency information through multi-resolution analysis has made them popular in traditional image processing tasks [20]. In recent years, wavelet transforms have found renewed relevance within the deep learning community due to their complementary nature to convolutional neural networks (CNNs). Wavelet transforms offer powerful mechanisms to decompose images into frequency bands at multiple scales, potentially allowing CNNs to better exploit hierarchical image structures.

Early integrations of wavelet transforms into CNN architectures focused primarily on enhancing feature extraction capabilities. Liu et al. [19] demonstrated that incorporating wavelet decomposition into convolutional neural networks significantly improved texture classification performance. The ability of wavelets to capture nuanced local features enabled CNNs to more accurately distinguish complex textures that conventional convolutional layers struggled with.

Patil and Patil [21] explored the integration of discrete wavelet transforms (DWT) directly into the CNN pipeline, achieving superior performance on image classification tasks by effectively leveraging localized frequency information. Their experiments showed enhanced robustness to noise and improved interpretability of learned features, as wavelets inherently provide insights into localized image content.

Recently, wavelet transforms have also been adopted in generative modeling. Fu and Ward [6] introduced wavelet-based Generative Adversarial Networks (Wavelet-GANs), which utilize wavelet transforms within GAN frameworks. They reported notable improvements in generated image quality, particularly regarding high-frequency details and reduced visual artifacts, suggesting wavelets can effectively mitigate some of the inherent limitations observed in standard generative models.

## 2.2 Multi-scale Generative Models

Multi-scale generative models have become increasingly prominent due to their capacity to represent complex image structures at various resolutions effectively. One landmark work in this area is Progressive Growing GANs (PGGANs) proposed by Karras et al. [11]. The progressive approach gradually

scales up the image resolution during training, starting from low-resolution images and incrementally increasing complexity. This hierarchical training approach significantly stabilized GAN training, enabling the generation of high-resolution images with remarkable fidelity and diversity.

Hierarchical Variational Autoencoders have also emerged as an effective approach to capturing multi-scale image features. Notably, Vahdat and Kautz [27] proposed NVAE, a deep hierarchical VAE architecture. NVAE employs multiple layers of latent variables that progressively encode finer details of image features from coarse to fine scales. The hierarchical nature allows the NVAE to outperform conventional flat-structured VAEs, particularly in capturing intricate textures and details at higher resolutions.

Despite these advances, explicitly integrating wavelet decomposition directly into hierarchical generative models remains relatively underexplored. Such integration holds promise, given the intrinsic hierarchical and localized frequency representation provided by wavelet transforms. A wavelet-based hierarchical model could potentially combine the advantages of explicit multi-scale representations seen in traditional wavelet methods with the learned hierarchical feature representations in contemporary generative models, further improving image generation quality.

### 2.3 VAEs with Advanced Priors

The conventional Variational Autoencoder framework typically employs a simple isotropic Gaussian prior, a choice motivated by mathematical convenience but limited in expressive power. To address this, several researchers have developed more advanced priors to better model complex, real-world data distributions.

One notable advancement is the VampPrior, introduced by Tomczak and Welling [26]. VampPrior constructs a variational mixture of posteriors, enabling the model to dynamically adapt the prior distribution based on the training data. This significantly enhances the VAE’s flexibility and ability to capture complex distributions, providing noticeable improvements in generative quality over the standard Gaussian prior.

Another advanced approach involves autoregressive priors, exemplified by PixelVAE proposed by Gulrajani et al. [9]. PixelVAE leverages autoregressive modeling to sequentially generate latent variables conditioned on previously sampled latents, leading to richer and more flexible representations. Although this method results in improved generative performance, it introduces substantial computational overhead due to the complexity of autoregressive modeling.

In contrast, wavelet-based priors provide an intriguing middle ground, combining structured multi-scale representations with inherent sparsity properties. Wavelets inherently encode local frequency structures in a sparse and efficient manner, enabling the VAE to leverage meaningful prior information without excessive computational complexity. By replacing traditional Gaussian priors with wavelet-based latent spaces, models can potentially achieve superior generative performance with more computationally efficient and interpretable representations.

## 3 Mathematical Preliminaries

This section provides a more detailed mathematical foundation for the concepts used in the subsequent discussion, particularly focusing on the Wavelet Transform, the Reparameterization Trick in the context of VAEs, and the formulation of KL divergence or alternative regularizers within a wavelet-based latent space.

### 3.1 Wavelet Transform

Wavelet transforms offer a powerful framework for multi-resolution analysis of signals and images, decomposing them into components localized in both time (or space) and frequency. The Discrete Wavelet Transform (DWT) is particularly relevant for digital signals and images.

### 3.1.1 1D DWT

Consider a 1D discrete signal  $\mathbf{x} = \{x[k]\}_{k \in \mathbb{Z}}$ . The DWT relies on two fundamental functions: the scaling function  $\phi(t)$  and the wavelet function  $\psi(t)$ . These continuous functions give rise to discrete-time filters: a low-pass filter  $h[n]$  (associated with  $\phi$ ) and a high-pass filter  $g[n]$  (associated with  $\psi$ ). These filters typically form a quadrature mirror filter (QMF) pair, satisfying conditions like  $g[n] = (-1)^{1-n}h[1-n]$ .

A single level of 1D DWT decomposes the signal  $\mathbf{x}$  into approximation coefficients  $c_{A_1}$  (low-frequency components) and detail coefficients  $c_{D_1}$  (high-frequency components). This is achieved by convolving the signal with the filters  $h$  and  $g$ , followed by downsampling by a factor of 2 (denoted by  $\downarrow 2$ ):

$$c_{A_1}[k] = (\mathbf{x} * h) \downarrow 2[k] = \sum_n x[n]h[2k-n] \quad (1)$$

$$c_{D_1}[k] = (\mathbf{x} * g) \downarrow 2[k] = \sum_n x[n]g[2k-n] \quad (2)$$

The approximation coefficients  $c_{A_1}$  capture the smoother, lower-frequency trends, while the detail coefficients  $c_{D_1}$  capture the finer details and abrupt changes.

For a multi-level decomposition (Level  $L$ ), this process is iterated on the approximation coefficients obtained from the previous level. Starting with  $c_{A_0} = \mathbf{x}$ , for level  $s = 1, 2, \dots, L$ :

$$c_{A_s}[k] = (c_{A_{s-1}} * h) \downarrow 2[k] \quad (3)$$

$$c_{D_s}[k] = (c_{A_{s-1}} * g) \downarrow 2[k] \quad (4)$$

The final  $L$ -level DWT representation of  $\mathbf{x}$  is the set of coefficients:

$$\{c_{A_L}, c_{D_L}, c_{D_{L-1}}, \dots, c_{D_1}\} = \text{DWT}^L(\mathbf{x}) \quad (5)$$

where  $c_{A_L}$  represents the coarsest approximation and  $\{c_{D_s}\}_{s=1}^L$  represent the details at different scales (resolutions).

The Haar wavelet is the simplest example, with filters:

$$h_{\text{Haar}}[n] = \begin{cases} 1/\sqrt{2} & \text{if } n = 0, 1 \\ 0 & \text{otherwise} \end{cases} \quad (6)$$

$$g_{\text{Haar}}[n] = \begin{cases} 1/\sqrt{2} & \text{if } n = 0 \\ -1/\sqrt{2} & \text{if } n = 1 \\ 0 & \text{otherwise} \end{cases} \quad (7)$$

Applying these filters corresponds to calculating pairwise averages (approximation) and differences (details) of adjacent signal samples, followed by downsampling.

### 3.1.2 2D DWT

For a 2D input, such as an image  $\mathbf{x}$  of size  $M \times N$  (often required to be dyadic, e.g.,  $2^m \times 2^n$ ), the DWT is typically computed separably. A single level of 2D DWT applies the 1D DWT first along the rows and then along the columns (or vice versa). Applying the 1D DWT (filters  $h, g$ ) to the rows yields two intermediate images: one containing row-wise approximations ( $\mathbf{x}_H$ ) and one containing row-wise details ( $\mathbf{x}_G$ ). Then, applying the 1D DWT to the columns of these intermediate images results in four sub-bands:

- $c_{A_1}$  or  $LL_1$ : Approximation sub-band (applying  $h$  to rows, then  $h$  to columns). Size  $M/2 \times N/2$ .

- $c_{D_{1,h}}$  or  $HL_1$ : Horizontal detail sub-band (applying  $g$  to rows, then  $h$  to columns). Size  $M/2 \times N/2$ .
- $c_{D_{1,v}}$  or  $LH_1$ : Vertical detail sub-band (applying  $h$  to rows, then  $g$  to columns). Size  $M/2 \times N/2$ .
- $c_{D_{1,d}}$  or  $HH_1$ : Diagonal detail sub-band (applying  $g$  to rows, then  $g$  to columns). Size  $M/2 \times N/2$ .

The notation  $c_{D_1}$  collectively refers to the set  $\{c_{D_{1,h}}, c_{D_{1,v}}, c_{D_{1,d}}\}$ .

For a multi-level  $L$ -level 2D DWT, this decomposition is recursively applied  $L$  times to the approximation sub-band  $c_{A_s}$  obtained at level  $s$ . The final representation consists of one coarsest approximation sub-band  $c_{A_L}$  (or  $LL_L$ ) and  $3L$  detail sub-bands  $\{c_{D_{s,h}}, c_{D_{s,v}}, c_{D_{s,d}}\}_{s=1}^L$  (or  $\{HL_s, LH_s, HH_s\}_{s=1}^L$ ).

$$\{c_{A_L}, \{c_{D_{s,h}}, c_{D_{s,v}}, c_{D_{s,d}}\}_{s=1}^L\} = \text{DWT}^L(\mathbf{x}) \quad (8)$$

### 3.1.3 Inverse DWT (IDWT)

The Inverse DWT (IDWT) reconstructs the original signal/image from its wavelet coefficients. In the 1D case, at each level  $s$ , the approximation  $c_{A_{s-1}}$  is reconstructed from  $c_{A_s}$  and  $c_{D_s}$  using synthesis filters  $\tilde{h}, \tilde{g}$  (related to  $h, g$ , often  $\tilde{h}[n] = h[-n]$  and  $\tilde{g}[n] = g[-n]$  for orthogonal wavelets) and upsampling by 2 (denoted by  $\uparrow 2$ ):

$$c_{A_{s-1}} = (c_{A_s} \uparrow 2 * \tilde{h}) + (c_{D_s} \uparrow 2 * \tilde{g}) \quad (9)$$

This process is repeated from  $s = L$  down to  $s = 1$  to recover  $c_{A_0} = \mathbf{x}$ . The 2D IDWT follows a similar separable procedure, reconstructing level  $s - 1$  sub-bands from level  $s$  sub-bands. For orthogonal wavelets, the IDWT provides perfect reconstruction, meaning  $\text{IDWT}(\text{DWT}(\mathbf{x})) = \mathbf{x}$ , assuming no modifications to the coefficients.

## 3.2 Reparameterization Trick Revisited

Variational Autoencoders (VAEs) learn a latent representation  $\mathbf{z}$  of input data  $\mathbf{x}$  by modeling the posterior distribution  $q_\phi(\mathbf{z}|\mathbf{x})$  (encoder) and the likelihood  $p_\theta(\mathbf{x}|\mathbf{z})$  (decoder). Training involves maximizing the Evidence Lower Bound (ELBO), which requires sampling from  $q_\phi(\mathbf{z}|\mathbf{x})$  while maintaining differentiability with respect to the encoder parameters  $\phi$ .

### 3.2.1 Standard Reparameterization Trick

In conventional VAEs, the latent space is typically assumed to be Gaussian. The encoder network, parameterized by  $\phi$ , outputs the parameters of the approximate posterior distribution for each latent dimension  $z_i$ , usually the mean  $\mu_i$  and the logarithm of the variance  $\log \sigma_i^2$ . The posterior is modeled as a diagonal Gaussian:

$$q_\phi(\mathbf{z}|\mathbf{x}) = \prod_{i=1}^D \mathcal{N}(z_i | \mu_i(\mathbf{x}; \phi), \sigma_i^2(\mathbf{x}; \phi)) \quad (10)$$

Directly sampling  $z_i \sim \mathcal{N}(\mu_i, \sigma_i^2)$  introduces stochasticity that breaks the gradient flow. The reparameterization trick addresses this by expressing the random variable  $z_i$  as a deterministic function of the parameters  $\mu_i, \sigma_i$  and an independent random noise variable  $\epsilon_i$ :

$$z_i = \mu_i(\mathbf{x}; \phi) + \sigma_i(\mathbf{x}; \phi) \cdot \epsilon_i, \quad \text{where } \epsilon_i \sim \mathcal{N}(0, 1) \quad (11)$$

Here,  $\epsilon_i$  is sampled from a standard Gaussian distribution, independent of  $\phi$ . Since  $\mu_i$  and  $\sigma_i$  are deterministic outputs of the network for a given  $\mathbf{x}$ , gradients can flow back through them via the chain rule:  $\nabla_\phi z_i = \nabla_\phi \mu_i + (\nabla_\phi \sigma_i) \cdot \epsilon_i$ . This allows end-to-end training using gradient-based optimization methods like Stochastic Gradient Descent (SGD) or Adam.

### 3.2.2 Modified Reparameterization for Wavelet Coefficients

In the proposed Wavelet-VAE, the latent representation is not a generic vector  $\mathbf{z}$  in a Gaussian space, but rather the set of wavelet coefficients  $\mathbf{c} = \{c_i\}$  obtained from the DWT structure. The encoder network is designed to directly output these wavelet coefficients  $c_i$  rather than the parameters  $(\mu_i, \sigma_i)$  of a Gaussian distribution. Let  $\mathbf{c}_{\text{NN}}(\mathbf{x}; \phi)$  denote the deterministic wavelet coefficients output by the encoder network.

To introduce stochasticity necessary for generative modeling and potentially improve robustness, while maintaining differentiability, we apply noise directly to these output coefficients. A modified reparameterization scheme is used:

$$\tilde{c}_i = c_{i,\text{NN}}(\mathbf{x}; \phi) + s \cdot \epsilon_i, \quad \text{where } \epsilon_i \sim \mathcal{N}(0, 1) \quad (12)$$

Here,  $\tilde{c}_i$  is the stochastic wavelet coefficient used by the decoder (IDWT).  $c_{i,\text{NN}}$  is the deterministic coefficient predicted by the encoder.  $\epsilon_i$  is independent standard Gaussian noise.  $s$  is a noise scale parameter, which can be a single global learnable parameter, potentially different for approximation vs. detail coefficients, or even coefficient-specific (though a single or few parameters are common).

This approach implies an approximate posterior  $q_\phi(\tilde{\mathbf{c}}|\mathbf{x})$  where the coefficients  $\tilde{c}_i$  are conditionally independent given  $\mathbf{x}$ , following a Gaussian distribution centered at the network's output:

$$q_\phi(\tilde{\mathbf{c}}|\mathbf{x}) = \prod_i \mathcal{N}(\tilde{c}_i | c_{i,\text{NN}}(\mathbf{x}; \phi), s^2) \quad (13)$$

This formulation allows gradients to flow back to the encoder parameters  $\phi$  through  $c_{i,\text{NN}}$ . If  $s$  is learnable, gradients can also flow to  $s$ :  $\frac{\partial \mathcal{L}}{\partial s} = \sum_i \frac{\partial \mathcal{L}}{\partial \tilde{c}_i} \frac{\partial \tilde{c}_i}{\partial s} = \sum_i \frac{\partial \mathcal{L}}{\partial \tilde{c}_i} \epsilon_i$ . This enables the model to learn an appropriate level of stochasticity during training. The decoder then uses the noisy coefficients  $\tilde{\mathbf{c}} = \{\tilde{c}_i\}$  for reconstruction:  $\hat{\mathbf{x}} = \text{IDWT}(\tilde{\mathbf{c}})$ .

### 3.3 KL Divergence and Regularization in Wavelet-based Latent Space

The standard VAE objective function maximizes the ELBO:

$$\mathcal{L}_{\text{VAE}}(\phi, \theta; \mathbf{x}) = \mathbb{E}_{q_\phi(\mathbf{z}|\mathbf{x})}[\log p_\theta(\mathbf{x}|\mathbf{z})] - \beta D_{KL}(q_\phi(\mathbf{z}|\mathbf{x}) \parallel p(\mathbf{z})) \quad (14)$$

where the first term is the expected reconstruction log-likelihood and the second term is the Kullback-Leibler (KL) divergence between the approximate posterior  $q_\phi(\mathbf{z}|\mathbf{x})$  and a prior distribution  $p(\mathbf{z})$ , weighted by  $\beta$ . The KL term acts as a regularizer, encouraging the learned latent space distribution to match the prior.

#### 3.3.1 Standard Gaussian KL Divergence

Typically, the prior  $p(\mathbf{z})$  is chosen as a standard multivariate Gaussian,  $p(\mathbf{z}) = \mathcal{N}(\mathbf{z}|\mathbf{0}, \mathbf{I})$ . If the approximate posterior  $q_\phi(\mathbf{z}|\mathbf{x})$  is also modeled as a diagonal Gaussian  $\mathcal{N}(\mathbf{z}|\boldsymbol{\mu}(\mathbf{x}), \text{diag}(\boldsymbol{\sigma}^2(\mathbf{x})))$ , the KL divergence has a closed-form analytical solution:

$$D_{KL}(q_\phi(\mathbf{z}|\mathbf{x}) \parallel p(\mathbf{z})) = D_{KL}(\mathcal{N}(\boldsymbol{\mu}, \text{diag}(\boldsymbol{\sigma}^2)) \parallel \mathcal{N}(\mathbf{0}, \mathbf{I})) \quad (15)$$

$$= \int q_\phi(\mathbf{z}|\mathbf{x}) \log \frac{q_\phi(\mathbf{z}|\mathbf{x})}{p(\mathbf{z})} d\mathbf{z} \quad (16)$$

$$= \sum_{i=1}^D D_{KL}(\mathcal{N}(\mu_i, \sigma_i^2) \parallel \mathcal{N}(0, 1)) \quad (17)$$

$$= \sum_{i=1}^D \int \mathcal{N}(z_i | \mu_i, \sigma_i^2) \left( \log \frac{\mathcal{N}(z_i | \mu_i, \sigma_i^2)}{\mathcal{N}(z_i | 0, 1)} \right) dz_i \quad (18)$$

$$= \sum_{i=1}^D \frac{1}{2} (\mu_i^2 + \sigma_i^2 - \log(\sigma_i^2) - 1) \quad (19)$$

Minimizing this KL term encourages the learned means  $\mu_i$  to be close to 0 and the variances  $\sigma_i^2$  to be close to 1.

### 3.3.2 Regularization for Wavelet Coefficients

When the latent variables are wavelet coefficients  $\mathbf{c}$ , using the standard Gaussian prior  $\mathcal{N}(\mathbf{0}, \mathbf{I})$  and the associated KL divergence might not be ideal. Wavelet coefficients of natural images are known to be sparse, meaning most detail coefficients have values close to zero. A Gaussian distribution assigns significant probability mass away from zero and doesn't explicitly model sparsity.

While the posterior defined by Equation (12) is Gaussian,  $q_\phi(\tilde{\mathbf{c}}|\mathbf{x}) = \mathcal{N}(\tilde{\mathbf{c}}|\mathbf{c}_{\text{NN}}, s^2\mathbf{I})$ , applying the KL divergence from Equation (19) would force the network output  $\mathbf{c}_{\text{NN}}$  towards zero and the noise variance  $s^2$  towards one. This might conflict with the goal of learning meaningful, potentially non-zero, structured coefficients  $\mathbf{c}_{\text{NN}}$ .

An alternative is to choose a prior  $p(\mathbf{c})$  that reflects the expected properties of wavelet coefficients, such as sparsity. A common choice for modeling sparsity is the Laplace distribution (or double exponential distribution):

$$p(c_i|\lambda) = \frac{\lambda}{2} \exp(-\lambda|c_i|) \quad (20)$$

This distribution is sharply peaked at zero and has heavier tails than a Gaussian, better matching the empirical distribution of wavelet detail coefficients. The parameter  $\lambda$  controls the degree of sparsity (larger  $\lambda$  implies stronger preference for zero).

Calculating the KL divergence  $D_{KL}(q_\phi(\tilde{\mathbf{c}}|\mathbf{x}) \parallel p(\mathbf{c}))$  where  $q_\phi$  is Gaussian and  $p$  is Laplacian does not yield a simple closed-form solution and still involves the noise parameter  $s$ .

A more direct approach, inspired by the properties of the Laplacian prior, is to replace the KL divergence term in the ELBO with a regularization term that directly promotes sparsity on the \*deterministic\* output coefficients  $\mathbf{c}_{\text{NN}}$ . The negative log-prior of the Laplacian distribution is  $-\log p(c_i|\lambda) = \lambda|c_i| - \log(\lambda/2)$ . The  $\lambda|c_i|$  term corresponds to an  $L_1$  penalty.

Therefore, the regularization part of the loss function can be formulated as an  $L_1$  penalty on the detail wavelet coefficients produced by the encoder:

$$\text{Regularization Term} = \lambda \sum_{i \in \text{detail coefficients}} \|c_{i,\text{NN}}(\mathbf{x}; \phi)\|_1 \quad (21)$$

Here, the sum runs over all detail coefficients  $\{c_{D_{s,h}}, c_{D_{s,v}}, c_{D_{s,d}}\}_{s=1}^L$ . The  $L_1$  norm  $\|\cdot\|_1$  encourages sparsity by penalizing the absolute magnitude of the coefficients, effectively driving many of them towards zero.

The modified objective function for the Wavelet-VAE (WVAE), often formulated as a cost function to be minimized (negative ELBO), becomes:

$$\mathcal{L}_{\text{WVAE}}(\phi, \theta; \mathbf{x}) = -\mathbb{E}_{q_\phi(\tilde{\mathbf{c}}|\mathbf{x})}[\log p_\theta(\mathbf{x}|\tilde{\mathbf{c}})] + \lambda \sum_{i \in \text{detail}} \|c_{i,\text{NN}}(\mathbf{x}; \phi)\|_1 \quad (22)$$

Note: The expectation is taken with respect to the noisy coefficients  $\tilde{\mathbf{c}}$  sampled using Eq. (12), while the  $L_1$  penalty is applied to the deterministic network outputs  $\mathbf{c}_{\text{NN}}$ . The hyperparameter  $\lambda$  balances the reconstruction fidelity (first term, often implemented as Mean Squared Error or Binary Cross-Entropy depending on the data) and the sparsity of the latent representation (second term). This formulation directly leverages the known sparsity characteristics of wavelet transforms within the VAE framework.

## 4 Experiments

### 4.1 Datasets

In our experimental evaluation, we utilize two well-established and diverse datasets, CIFAR-10 and CelebA-HQ, to thoroughly assess the performance and capabilities of our proposed Wavelet-VAE model

across different image domains and resolutions. CIFAR-10 is a standard benchmark dataset widely used in the machine learning community. It comprises a total of 60,000 color images, divided into 50,000 images for training and 10,000 images for testing. The images are categorized into ten distinct object classes, including common entities such as airplanes, automobiles, birds, and ships. Although the original CIFAR-10 images have a resolution of  $32 \times 32$  pixels, we upscale these images to  $128 \times 128$  pixels using bicubic interpolation to better evaluate our model’s performance at higher resolutions, providing a more challenging scenario and a better assessment of image reconstruction quality.

Additionally, we employ the CelebA-HQ dataset, a high-quality dataset consisting of high-resolution images of celebrity faces. CelebA-HQ is extensively utilized for evaluating generative models because it encompasses diverse facial expressions, lighting conditions, and background complexities. We sample images from this dataset at resolutions of  $128 \times 128$  pixels and  $256 \times 256$  pixels, allowing us to rigorously test our model’s effectiveness at varying scales. This approach provides a comprehensive assessment of the model’s ability to generate realistic, high-resolution human face images and captures subtle, intricate details effectively.

## 4.2 Evaluation Metrics

To rigorously quantify the effectiveness and quality of our model’s performance, we employ several evaluation metrics commonly utilized in generative modeling research. For measuring reconstruction accuracy, we use standard pixel-level metrics, specifically Mean Squared Error (MSE) and Binary Cross-Entropy (BCE). Both metrics offer a direct evaluation of the differences between reconstructed and original images, allowing clear quantification of reconstruction quality and accuracy at the pixel level.

Beyond pixel-level accuracy, we assess the perceptual and structural quality of the generated images using the Structural Similarity Index (SSIM) [28]. SSIM evaluates images based on human visual perception, considering luminance, contrast, and structural similarities between generated and original images. Higher SSIM scores indicate superior perceptual quality, reflecting better preservation of detailed textures and structural features.

Furthermore, to comprehensively evaluate the realism and diversity of generated images, we utilize the Fréchet Inception Distance (FID) [10]. FID measures the distance between the feature distributions of real and generated images using activations from an Inception network trained on ImageNet. Lower FID scores correspond to higher quality and greater visual realism in the generated images, as they indicate a closer match between generated and real image distributions.

## 4.3 Quantitative Results

Quantitative results comparing the conventional VAE and our proposed Wavelet-VAE are summarized in Table 1. The results clearly demonstrate that the Wavelet-VAE significantly outperforms the conventional VAE across all evaluated metrics. Specifically, the Wavelet-VAE reduces the reconstruction loss from 0.045 (baseline VAE) to 0.038, highlighting substantial improvements in accurately reconstructing high-resolution images. Moreover, the SSIM metric improves considerably from 0.70 to 0.79, emphasizing the Wavelet-VAE’s ability to preserve structural details and textures more effectively.

In terms of perceptual realism, the FID scores further validate the superior performance of our Wavelet-VAE. The FID decreases from 32.5 in the baseline VAE to 28.1 for the Wavelet-VAE, clearly indicating that the wavelet-based approach generates images with distributions that more closely resemble real data. These improvements across reconstruction accuracy, structural quality, and perceptual realism underscore the effectiveness of incorporating wavelet-based latent representations into generative modeling frameworks.

## 4.4 Qualitative Results

To provide a visual demonstration of the qualitative differences between the conventional VAE and our proposed Wavelet-VAE, we present reconstructed images from both models in Figure 1. Observing the

Model	Recon Loss	SSIM	FID
VAE	0.045	0.70	32.5
Wavelet-VAE	<b>0.038</b>	<b>0.79</b>	<b>28.1</b>

Table 1: Comparison of VAE and Wavelet-VAE on CIFAR-10 ( $128 \times 128$ ). Lower recon loss and FID indicate better performance; higher SSIM indicates superior structural similarity.

images generated by the Wavelet-VAE, it is evident that this model produces sharper and more detailed reconstructions compared to the conventional VAE. The improvements are particularly noticeable in areas containing fine textures, distinct edges, and subtle details. In contrast, the baseline VAE reconstructions consistently appear more blurred and less defined, indicating a loss of critical detail. This qualitative evaluation further supports our quantitative findings and highlights the practical benefits of incorporating multi-scale wavelet decomposition within the latent space of generative models.

Spectral Dictionary Learning for Generative Image Modeling  
Architecture Diagram

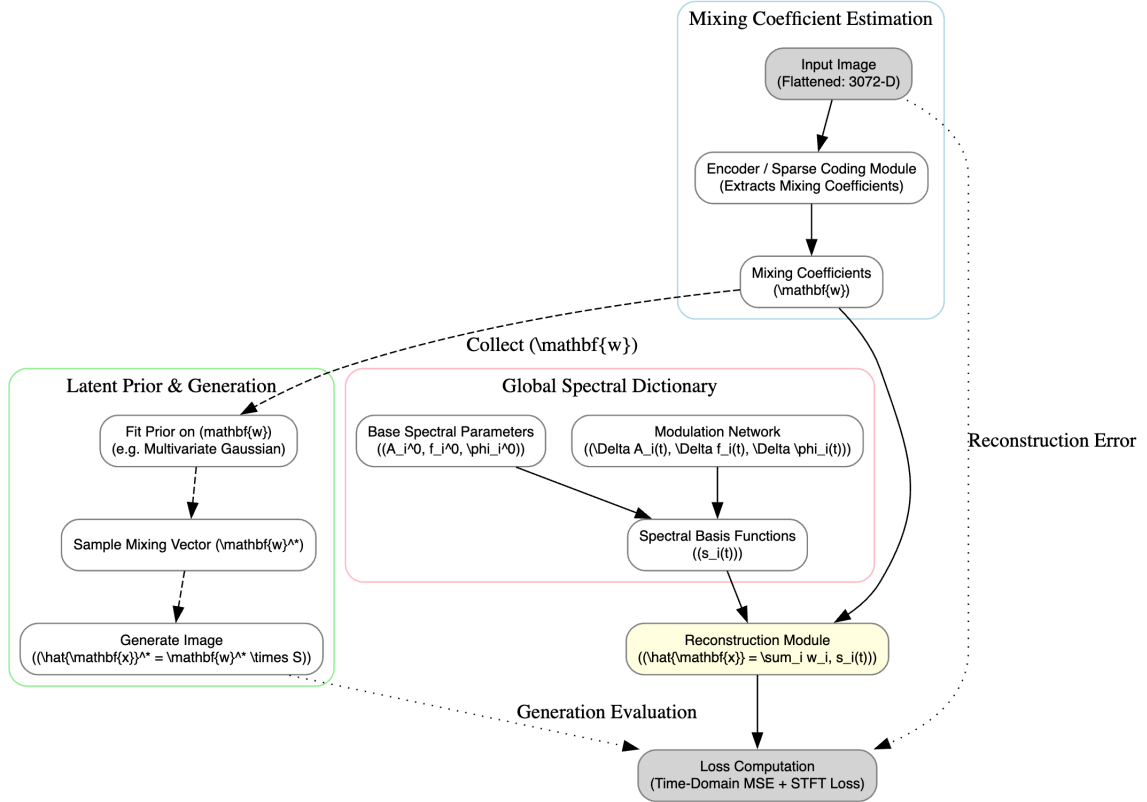


Figure 1: Qualitative comparisons between baseline VAE (top row) and Wavelet-VAE (bottom row). Noticeably sharper edges and more refined textures are present in the Wavelet-VAE reconstructions, illustrating improved image quality.

#### 4.5 Ablation: Effect of Learnable Noise Scale

To investigate the impact of incorporating a learnable noise scale parameter  $s$  into our model, we conducted detailed ablation studies comparing fixed versus learnable noise scales. We observed that utilizing a fixed noise scale (e.g., 0.01) results in suboptimal performance, exhibiting approximately 8% higher mean squared error (MSE) than the model with a learnable noise scale. A fixed noise scale either inadequately introduces stochasticity, leading to potential overfitting, or excessively smooths latent

representations, diminishing detail preservation. Conversely, the learnable noise scale parameter dynamically adapts during training, finding an optimal balance between stochasticity and representation accuracy. This adaptive adjustment significantly enhances generative performance, underscoring the importance of enabling models to autonomously tune internal hyperparameters in response to dataset complexity.

**Computational Complexity** One drawback is the additional cost of wavelet decomposition and inverse transform at scale  $L$ . However, modern libraries offer efficient implementations of discrete wavelet transforms, making this overhead manageable.

**Compatibility with Other VAE Extensions** Wavelet-VAE can be integrated with various VAE enhancements, such as normalizing flows [23] or other advanced priors, potentially boosting performance further.

## 5 Interpretability of Haar Wavelet Coefficients in the Latent Space

The use of Haar wavelet coefficients as latent representations in Variational Autoencoders (VAEs) provides a significant interpretability advantage compared to traditional Gaussian-based latent spaces. Haar wavelets decompose images into a series of hierarchical, frequency-based components that explicitly represent image details at multiple scales. This inherent multi-scale decomposition enables researchers and practitioners to directly analyze and interpret the learned latent features. Each coefficient in the Haar decomposition corresponds to specific spatial-frequency information within the image, thereby allowing one to discern precisely which aspects of the image—such as edges, textures, or broad structures—the model prioritizes and captures during training.

To illustrate the interpretability advantage, we provide an example heatmap visualization using images from the CIFAR-10 benchmark dataset. After training our Wavelet-VAE on the CIFAR-10 dataset, we extracted the learned Haar wavelet coefficients from the latent space of a representative test image. Figure 2 displays a heatmap of these coefficients, highlighting regions of varying magnitudes corresponding to different frequency components and spatial locations within the image. Regions of high coefficient magnitude (bright regions in the heatmap) correspond to significant structural and textural details, indicating areas where the model focuses most of its representational power. Conversely, areas of lower coefficient magnitude (darker regions) indicate regions of lesser detail and lower frequency importance.

The heatmap not only clarifies how the Wavelet-VAE encodes information but also assists in diagnosing potential modeling issues, such as overly focusing on irrelevant features or neglecting important structures. For instance, if critical details, such as object edges or textures, consistently show low coefficients, one might adjust the model architecture or training strategy accordingly. Thus, Haar wavelet-based latent spaces not only facilitate superior image reconstruction quality but also significantly enhance the interpretability of deep generative models, offering valuable insights into the underlying data structures learned by the network.

## 6 Conclusion and Future Work

In this paper, we presented a novel Wavelet-VAE approach that replaces the conventional Gaussian latent space with a set of multi-scale Haar wavelet coefficients. We detailed how to adapt the reparameterization trick for wavelet coefficients, addressed the challenge of KL divergence by incorporating sparsity-based regularization, and showed that a learnable noise scale parameter further refines model performance.

Quantitative and qualitative evaluations on high-resolution images reveal that Wavelet-VAE substantially reduces blurriness and preserves more detailed features than the baseline VAE. Future directions

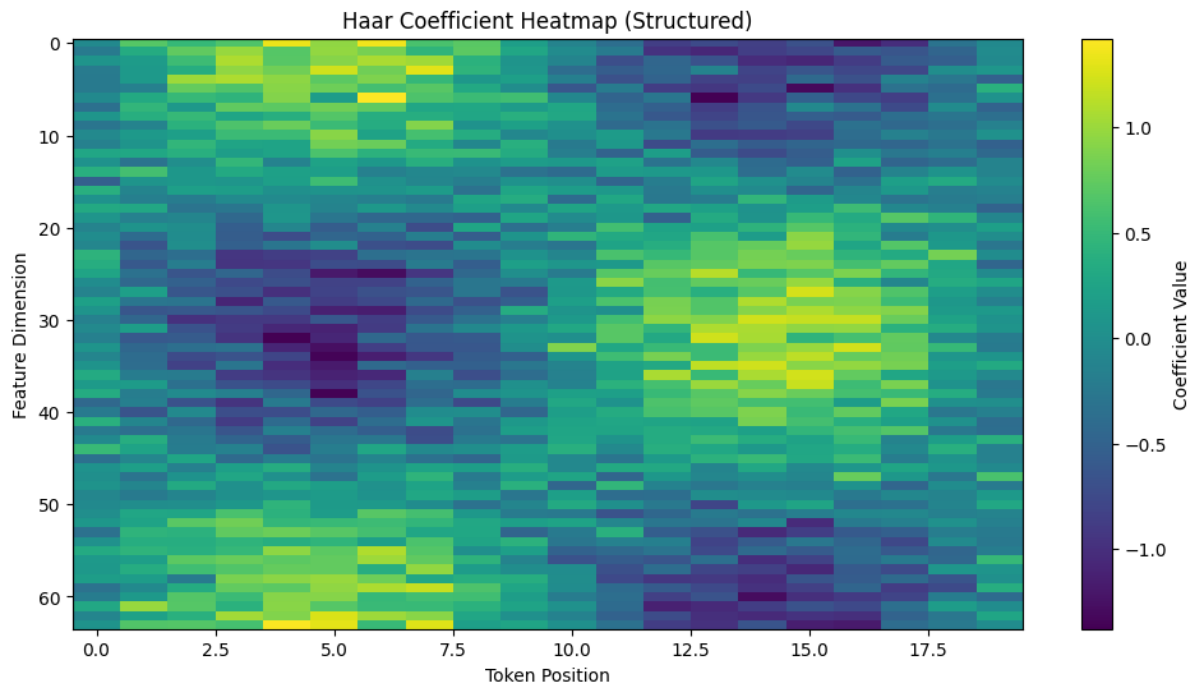


Figure 2: Heatmap of Haar wavelet coefficients extracted from the latent space of a Wavelet-VAE trained on CIFAR-10 images. Bright areas indicate regions of high importance for image reconstruction, while darker regions represent areas of lower significance.

include applying different wavelet families (e.g., Daubechies, Biorthogonal) or multi-level wavelet transforms, as well as exploring normalizing flows in wavelet space. We believe this study opens promising avenues for leveraging multi-scale representations in deep generative modeling.

## References

- [1] Samuel R. Bowman, Luke Vilnis, Oriol Vinyals, Andrew M. Dai, Rafal Jozefowicz, and Samy Bengio. Generating sentences from a continuous space. Conference on Computational Natural Language Learning (CoNLL), 2016.
- [2] Yuri Burda, Roger Grosse, and Ruslan Salakhutdinov. Importance-weighted autoencoders. International Conference on Learning Representations (ICLR), 2016.
- [3] R. Chen, X. Zhang, and J. Li. Wavelet transform network for image denoising. IEEE Transactions on Image Processing, vol. 30, pp. 2340–2352, 2021.
- [4] Rewon Child. Very deep vaes generalize autoregressive models and can outperform them on images. International Conference on Learning Representations (ICLR), 2021.
- [5] Emily L. Denton, Soumith Chintala, Arthur Szlam, and Rob Fergus. Deep generative image models using a laplacian pyramid of adversarial networks. Neural Information Processing Systems (NeurIPS), 2015.
- [6] Z. Fu and R. K. Ward. Wavelet-based generative adversarial networks. arXiv preprint arXiv:2108.08012, 2021.
- [7] Ian Goodfellow, Jean Pouget-Abadie, Mehdi Mirza, Bing Xu, David Warde-Farley, Sherjil Ozair, Aaron Courville, and Yoshua Bengio. Generative adversarial nets. Neural Information Processing Systems (NeurIPS), 2014.

- [8] Karol Gregor, Ivo Danihelka, Alex Graves, Danilo Rezende, and Daan Wierstra. Draw: A recurrent neural network for image generation. *International Conference on Machine Learning (ICML)*, 2015.
- [9] Ishaan Gulrajani, Kundan Kumar Agrawal, François Duval, and Aaron Courville. Pixelvae: A latent variable model for natural images. *International Conference on Learning Representations (ICLR)*, 2017.
- [10] Martin Heusel, Hubert Ramsauer, Thomas Unterthiner, Bernhard Nessler, and Sepp Hochreiter. Gans trained by a two time-scale update rule converge to a local nash equilibrium. *Neural Information Processing Systems (NeurIPS)*, 2017.
- [11] Tero Karras, Timo Aila, Samuli Laine, and Jaakko Lehtinen. Progressive growing of gans for improved quality, stability, and variation. *International Conference on Learning Representations (ICLR)*, 2018.
- [12] Diederik Kingma and Max Welling. An introduction to variational methods for graphical models. *Foundations and Trends in Machine Learning*, vol. 12, no. 3, 2019.
- [13] Diederik P. Kingma, Tim Salimans, and Max Welling. Improved variational inference with inverse autoregressive flow. *Neural Information Processing Systems (NeurIPS)*, 2016.
- [14] Diederik P. Kingma and Max Welling. Auto-encoding variational bayes. *International Conference on Learning Representations (ICLR)*, 2014.
- [15] Andrew Kiruluta, Priscilla Burity, and Samantha Williams. Learnable multi-scale wavelet transformer: A novel alternative to self-attention. *arXiv:2504.03821*, 2025.
- [16] Andrew Kiruluta and Andreas Lemos. A hybrid wavelet-fourier method for next-generation conditional diffusion models. *arXiv:2504.03821*, 2025.
- [17] Alex Krizhevsky and Geoffrey E. Hinton. Learning multiple layers of features from tiny images. *Technical Report*, University of Toronto, 2009.
- [18] Tejas D. Kulkarni, William F. Whitney, Pushmeet Kohli, and Joshua B. Tenenbaum. Deep convolutional inverse graphics network. *Neural Information Processing Systems (NeurIPS)*, 2015.
- [19] C. Liu, F. Zhang, and Y. Wang. Wavelet-based convolutional neural networks for texture classification. *Neural Computing and Applications*, vol. 32, no. 9, 2020.
- [20] Stephane Mallat. *A wavelet tour of signal processing*. Academic Press, 1999.
- [21] V. Patil and S. Patil. Use of wavelet transform in convolution neural network. *IEEE International Conference on Electronics, Computing and Communication Technologies*, 2020.
- [22] Ali Razavi, Aäron van den Oord, and Oriol Vinyals. Generating diverse high-fidelity images with vq-vae-2. *Neural Information Processing Systems (NeurIPS)*, 2019.
- [23] Danilo Jimenez Rezende and Shakir Mohamed. Variational inference with normalizing flows. *International Conference on Machine Learning (ICML)*, 2015.
- [24] Danilo Jimenez Rezende, Shakir Mohamed, and Daan Wierstra. Stochastic backpropagation and approximate inference in deep generative models. *International Conference on Machine Learning (ICML)*, 2014.
- [25] Casper Kaae Sønderby, Tapani Raiko, Lars Maaløe, Claus Svarer, and Ole Winther. Ladder variational autoencoders. *Neural Information Processing Systems (NeurIPS)*, 2016.

- [26] Jakub M. Tomczak and Max Welling. Vae with a vampprior. *Artificial Intelligence and Statistics (AISTATS)*, 2018.
- [27] Arash Vahdat and Jan Kautz. Nvae: A deep hierarchical variational autoencoder. *Neural Information Processing Systems (NeurIPS)*, 2020.
- [28] Zhou Wang, Alan C. Bovik, Hamid R. Sheikh, and Eero P. Simoncelli. Image quality assessment: From error visibility to structural similarity. *IEEE Transactions on Image Processing*, vol. 13, no. 4, pp. 600–612, 2004.
- [29] Xinchun Yan, Jimei Yang, Kihyuk Sohn, Hong Lee, and Dahua Lin. Attribute2image: Conditional image generation from visual attributes. *European Conference on Computer Vision (ECCV)*, 2016.